Adsorption 11: 449–454, 2005

Adsorption and Diffusion of N_2 and O_2 in LiLSX Studied by Neutron Scattering Techniques

HERVE JOBIC*
Institut de Recherches sur la Catalyse, CNRS, 2 avenue Albert Einstein, 69626 Villeurbanne, France
jobic@catalyse.cnrs.fr

HELMUT SCHOBER
Institut Laue-Langevin, BP 156, 38042 Grenoble, France

PLUTON PULLUMBI
Air Liquide, Centre de Recherche Claude Delorme, B.P. 126, Les Loges-en-Josas, 78354 Jouy-en-Josas, France

Abstract. The vibrational frequencies and diffusivities of N_2 and O_2 adsorbed in LiLSX have been studied by neutron scattering. Experiments were performed with the single components at 260 K, at various loadings. The stretching frequency of N_2 in interaction with Li cations, as observed by inelastic neutron scattering, is compared with quantum chemical calculations. The transport diffusivities of N_2 and O_2 are derived from quasi-elastic neutron scattering, O_2 diffusing faster than N_2. The Darken approximation is found to be inexact, the corrected diffusivities of O_2 and N_2 decreasing with increasing loading.

Keywords: diffusion, nitrogen, oxygen, LiLSX, neutron scattering

1. Introduction

Air separation for oxygen production is an important operation in the chemical processing industry as well as in energy conversion applications. Classical cryogenic air separation is gradually giving way to new technologies involving either Pressure Swing Adsorption (PSA), Vacuum Swing Adsorption (VSA) or membrane permeation. In addition to the operating parameters of the process itself, important factors influencing the performance of the production unit are the adsorption properties of the adsorbent material as well as N_2 and O_2 transport properties through the bed.

The separation of N_2 and O_2 is performed in cation-containing zeolites. The higher permanent quadrupole moment of N_2 compared to that of O_2 is the main cause of their thermodynamic separation due to their difference in interaction with the extra-framework cations. As quantum-chemical studies of zeolites used for gas separation must treat very large unit cells, fully periodic ab initio simulations are unfortunately not yet practical due to large CPU time requirements. Embeded and hybrid QM/MM methods can be used to study the behavior of adsorbed molecules within zeolitic materials including the effect of the field and field gradient upon adsorption energies.

Previous works on this system concern essentially structural and sorption equilibrium aspects (Plevert et al., 1997; Feuerstein and Lobo, 1998; Jale et al., 2000; De Luca et al., 2001; Pullumbi et al., 1999). The diffusion of N_2 and O_2 in LiLSX has not been yet studied by microscopic methods, although the diffusion of N_2 in NaX and NaCaA was measured by pulsed-field gradient NMR (PFG NMR) (Bär et al., 1997). We report here neutron scattering measurements of N_2 and O_2 in LiLSX. Hydrogen is traditionally the best probe for

*To whom correspondence should be addressed.

neutrons, because of its large scattering cross section. With the high neutron flux available on recent spectrometers, the adsorption and diffusion of molecules which do not contain hydrogen atoms can also be followed by neutron scattering. For N_2 interacting with Li cations, a sensitive test of the calculations is the N_2-Li stretching frequency. This vibrational mode occurs at low frequency so that it cannot be observed directly by optical techniques. However, it can be measured by inelastic neutron scattering (INS). The diffusion coefficients of N_2 and O_2 can be derived from the broadening of the spectra around zero energy transfer, hence the name of the technique: quasi-elastic neutron scattering (QENS).

There are two objectives in the present work: (a) to determine the vibrational frequency of N_2 interacting with Li cations in LiLSX, by INS and quantum chemical methods, and (b) to obtain by QENS the transport and corrected diffusivities of N_2 and O_2 in this zeolite.

2. Experimental and Calculation Methods

2.1. Neutron Scattering

The QENS experiments were performed at the Institut Laue-Langevin, Grenoble, using the spectrometer IN6. This instrument has a high flux, thanks to vertical and time focusing. This is crucial, considering the relatively small coherent cross sections of nitrogen (11 barns) and oxygen (4.2 barns) atoms compared with the incoherent cross section of hydrogen (80 barns).

The LiLSX was activated by heating up to 723 K under vacuum. The N_2 and O_2 loadings were determined from the equilibrium pressures and from the experimental adsorption isotherms measured at the same temperature as the QENS experiment: 260 K. Although the diffusion of N_2 could have been measured at 300 K, a lower temperature was selected to increase the signal of O_2, which has a lower cross section and is much less adsorbed than N_2.

2.2. Theoretical Models and Calculation Methods

Faujasite (FAU) crystallizes in the cubic space group *Fd3m*, with a lattice constant ranging from about 24.2 to 25.1 Å, depending on the framework aluminium concentration, cations, and state of hydration. There are 192 tetrahedral sites per unit cell. Low silica Faujasites (LSX) are composed of the same number of silica and alumina tetrahedra. One of the main difficulties in accurately modelling adsorption in zeolites lies in providing an adequate treatment of each cation and its environment. The problem is two-fold: first, an accurate model of the cation-adsorbate molecule must be used and second, long-range interactions of the environment (steric constraints and Madelung field) on the model must be included.

The structure of LiLSX, space group $Fd\bar{3}$, has been constructed from experimental data reported recently (Plevert et al., 1997). The QM/MM method has been previously used for studying adsorption of gaseous molecules in zeolitic frameworks (De Luca et al., 2001; Pullumbi et al., 1999; Tielens and Geerlings, 2001). In this study we have adopted a different methodology from the one reported in Pullumbi et al. (1999). Here we calculate the interaction energy of the gas molecules with each accessible Li cation. The embedded cluster approach consists of a Li^+-molecule (N_2 or O_2) system treated quantum chemically, surrounded by the specific environment of each cationic site, i.e. point charges simulating the Al, Si, O, and Li^+ zeolite ions by reconstructing the LiLSX unit cell with each of the cations of quantum part at the centre of the cell followed by the removal of periodic boundary conditions. This methodology allows us to take into account long-range effects (the electrostatic field generated by all the atoms of the cell at the position of the isolated QM part), which differs from one cation to another. The electrostatic field strongly affects the optimised geometry and the vibrational frequency of the QM part. For this reason, the reconstruction of the cell with each quantum cation located at its center avoids erroneous estimations of the electrostatic field due to the border region truncation. The QM calculations have been performed within the framework of the density functional theory (DMol) and gradient-corrected potential and energy functionals have been used for exchange (Becke, 1988) and correlation (Perdew, 1986). Technical details of the electrostatic embedding are described in De Luca et al. (2001) and Pullumbi et al. (1999). As discussed in these papers, this method needs as inputs the values of the charges representing the zeolite atoms. At first sight, this is not a trivial problem, since charges are not directly measurable properties. The embedding charges used in this study, i.e. Si (+2.4), Al (+1.4), O (−1.2), and Li (+1.0), are those used for GCMC simulations. The QM lithium cations were also assumed to bear $a + 1$ charge neglecting thus any zeolite to cation charge transfer.

3. Results and Discussion

3.1. Vibrations

The interaction of N_2 with Li cations is evidenced by inelastic neutron scattering (INS) results. A vibration is measured around 13 cm^{-1} when N_2 was adsorbed in LiLSX (Fig. 1), whereas no band is observed upon O_2 adsorption. In another study performed in silicalite (Papadopoulos et al., 2004) no vibration was found after N_2 adsorption. These results indicate that the band centred at 13 cm^{-1} is specific to the interaction Li-nitrogen. Taking into account the adsorption geometry (end-on), this vibrational feature is assigned to the stretching vibration of the adsorption complex. From the loading dependence of the INS spectra (Fig. 1), it appears that this band has a maximum intensity around 3 nitrogen molecules per supercage, so that all Li cations do not act as adsorption sites for N_2. Upon increasing the loading, the width of this band becomes larger than the instrumental resolution, indicating a distribution of interaction energies.

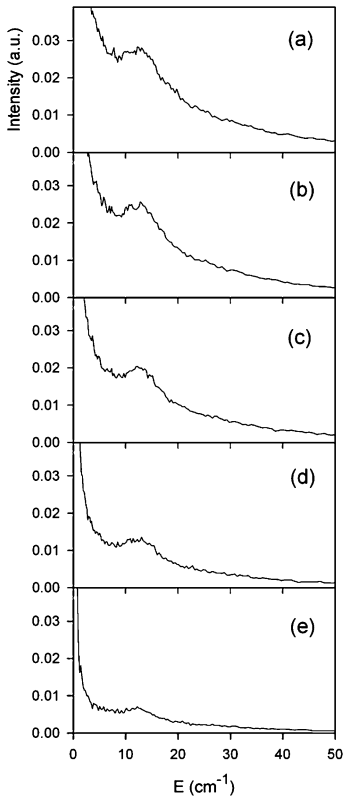

Figure 1. Inelastic neutron scattering spectra obtained for N_2 in LiLSX at 260 K, for different concentrations: (a) 3.68, (b) 3.27, (c) 2.62, (d) 1.59, (e) 0.78 molecule/supercage ($Q = 1.19$ Å^{-1}).

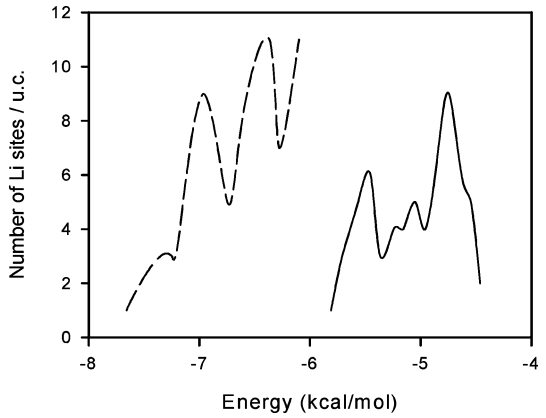

Figure 2. Interaction energy distributions of Li-N_2 (dashed line) and Li-O_2 (full line) for all accessible cations in LiLSX.

Out of the 96 cations of the LiLSX zeolite, 32 are located in sites I' which are completely inaccessible. The 64 remaining cations are distributed between sites II, III and III'. The distribution of interaction energies of N_2 and O_2 with the Li cation, calculated as described above, is reported in Fig. 2. It is clear that the binding of nitrogen is significantly higher than that of oxygen. As there are 8 supercages/u.c., and following the INS results, it appears that the adsorption sites correspond to the first peak on this figure (-7.7 to -6.8 kcal/mol). In Fig. 3, the calculated Li-N_2 vibrational frequencies have been reported for each site. The observable trend is that there is a correlation of the interaction energy with the frequency of the Li-N_2 stretching. This is consistent with the well-known trend of strong inverse linear relationship between the calculated molecular

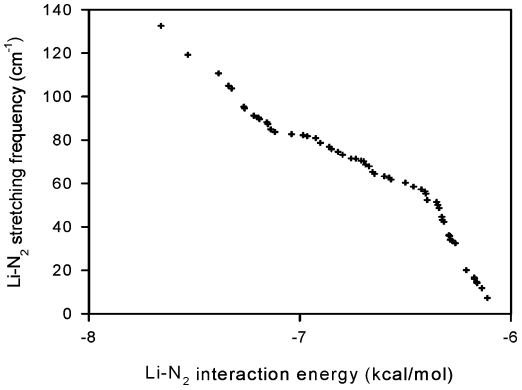

Figure 3. Calculated Li-N_2 vibrational frequencies for all accessible cations in LiLSX.

electrostatic potentials (electrostatic field) at the active site and the internal stretching frequency of the coordinated ligand (in our case N-N stretch) and an inverse relationship between cation-ligand frequency (in our case Li-N stretch). The fact that the vibrational stretching frequencies are very sensitive to the electrostatic field clearly indicates that the representation of the electrostatic field within the zeolite using partial charges on all the atoms of the unit cell is only an approximation and could be improved using more realistic representations such as frozen electron densities.

3.2. *Diffusion*

Most of the QENS measurements are performed on hydrogenated molecules, since the large incoherent cross section of hydrogen gives a good contrast with the signal from the zeolite. From these experiments, self-diffusivities could be derived. However, one can also probe the diffusion of coherent scatterers, such as N_2 and O_2. One can extract in this case the transport diffusivity (Jobic et al., 1999; Papadopoulos et al., 2004).

Some of the QENS spectra obtained for N_2 at three different loadings are shown in Fig. 4. The broadening of the elastic peak, hence the transport diffusivity, increases slightly with increasing loading. Due to the lower scattering cross section of O_2, and to its smaller concentration, only two loadings were studied (Fig. 5). The broadenings are larger than in the case of N_2. Contrary to N_2, the transport diffusivity is larger at the lowest loading.

All the spectra were first fitted individually with a Lorentzian function, corresponding to diffusion, convoluted with the instrumental resolution. The widths obtained for N_2 at the different loadings are plotted in Fig. 6 as a function of Q^2. This broadening behaviour is characteristic of jump diffusion. The spectra obtained at a given occupancy could be fitted simultaneously with a jump diffusion model having a fixed jump length. The transport diffusion coefficients, D_t, which are derived from the refinements are shown in Fig. 7. The transport diffusivity of N_2 increases with increasing loading, but the reverse trend is observed for O_2. In the experimental conditions used ($P \leq 1$ atm), the transport diffusivity of O_2 is always larger than the one of N_2. The absolute error estimated for the diffusion coefficients is 50%. However, the relative error is less than 20%, since the same treatment is applied to all raw data.

The corrected diffusivities, D_0, were obtained by correcting the transport diffusivities from the thermodynamic factor, calculated from the adsorption isotherms (Fig. 8). These quantities are linked by the so-called Darken equation

$$D_t(\theta) = D_0(\theta)\left(\frac{d\ln p}{d\ln c}\right) \qquad (1)$$

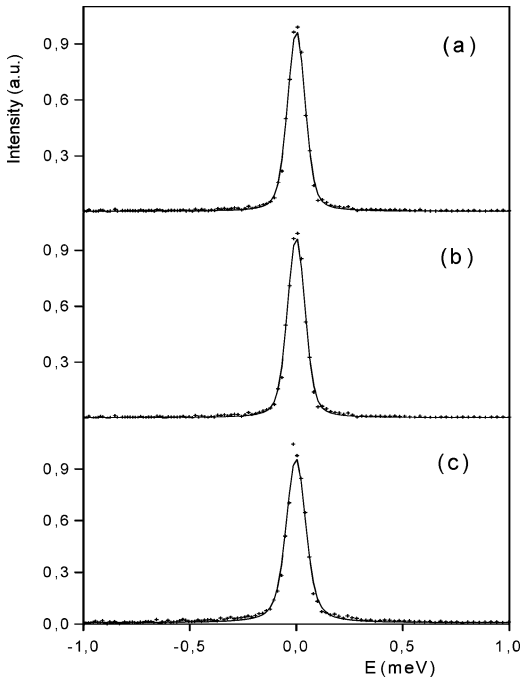

Figure 4. Comparison between experimental (crosses) and calculated (solid lines) QENS spectra obtained for N_2 in LiLSX at 260 K, for different concentrations: (a) 0.78, (b) 2.62, and (c) 3.68 molecules per supercage ($Q = 0.24$ Å^{-1}).

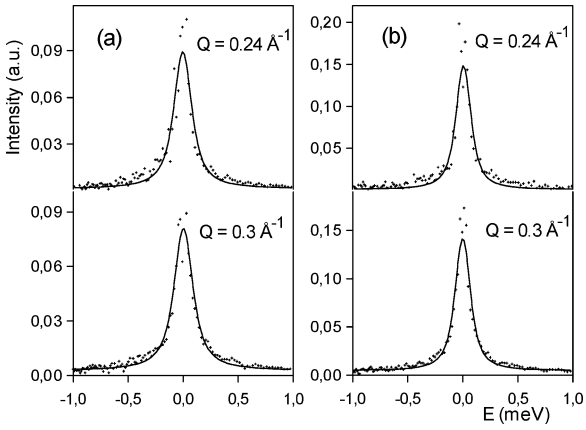

Figure 5. Comparison between experimental (crosses) and calculated (solid lines) QENS spectra obtained for O_2 in LiLSX at 260 K: (a) 0.53 molecule/supercage; (b) 0.7 molecule/supercage.

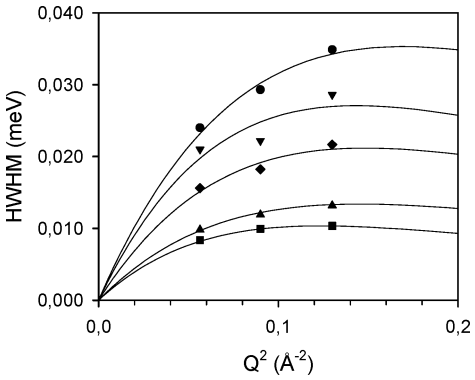

Figure 6. Broadenings obtained for N_2 in LiLSX at 260 K, for different loadings: (■) 0.78, (▲) 1.59, (♦) 2.62, (▼) 3.27, (●) 3.68 molecules/supercage.

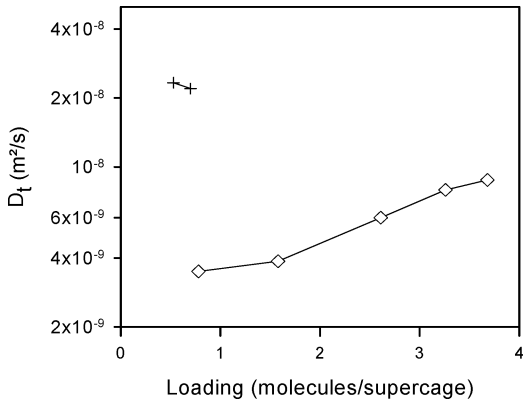

Figure 7. Transport diffusivities of N_2 (◇) and O_2 (+) in LiLSX obtained by QENS at 260 K.

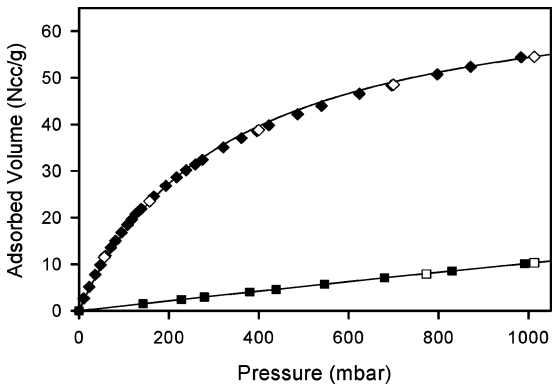

Figure 8. Experimental adsorption isotherms for N_2 (♦) and O_2 (■) in LiLSX at 260 K; the open symbols correspond to the QENS measurements.

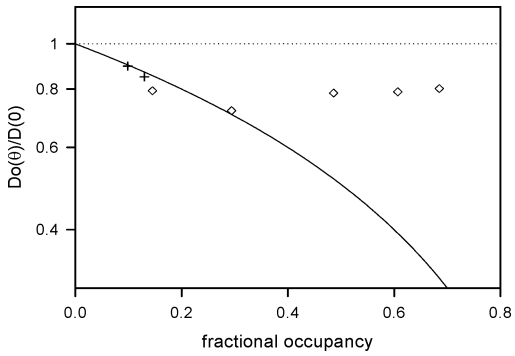

Figure 9. Normalised corrected diffusivities of N_2 (◇) and O_2 (+) in LiLSX at 260 K, as a function of fractional occupancy. The solid line corresponds to a $(1 - \theta)$ dependence.

The normalised corrected diffusivities are shown in Fig. 9 as a function of loading, they are decreasing slightly more rapidly in the case of O_2 than for N_2. The loading dependence of the diffusivity of O_2 could be studied in a larger range from new measurements at a lower temperature, where higher loading could be attained. The decrease of the corrected diffusivities for increasing fractional occupancy can be related to attractive forces between the molecules (Paschek and Krishna, 2001; Papadopoulos et al., 2004).

The activation energy for diffusion was determined only for nitrogen, for a loading of 2 molecules/supercage. The diffusivity obtained at 293 K is of 8.7×10^{-9} m^2 s^{-1}. The activation energy estimated from the two temperatures is of 11 KJ/mol. This is much larger than the value obtained in silicalite, 2.7 KJ/mol (Papadopoulos et al., 2004), which reflects the interaction with the Li cations, as observed by INS. The activation energy we obtain in LiLSX is comparable to the values measured in NaX, 10.8 KJ/mol, and in NaCaA, 8.5 KJ/mol (Bär et al., 1997).

At zero loading, the transport and self-diffusivities should be equal so that one can compare the value obtained for N_2 at 260 K at the lowest loading, 3.5×10^{-9} m^2 s^{-1}, to the data obtained by PFG NMR. However for N_2, the PFG NMR intracrystalline diffusivities tend to approach a limiting value between 200 and 300 K, about 10^{-9} m^2 s^{-1}, which was attributed to a loading variation within the NMR tube (Bär et al., 1997). One does not observe such a plateau in our measurements performed at finite loadings, and we can derive an activation energy in this temperature range. The QENS results for N_2 and O_2 in LiLSX are in agreement with the faster intracrystalline diffusion measured

by ZLC for O_2, compared with N_2 (Ruthven and Xu, 1993). A ZLC experiment measures the limiting transport diffusivity at low loading. The ZLC intracrystalline diffusivities extrapolated to 300 K are of the order of 10^{-10} m^2 s^{-1}, which is almost two orders of magnitude smaller than the QENS or PFG NMR (Bär et al., 1997) values. Such a discrepancy between microscopic and macroscopic data has already been observed for several zeolitic systems (Kärger and Ruthven, 1992).

4. Conclusions

The adsorption and diffusion of almost any adsorbed gas can now be characterized by neutron scattering techniques. In LiLSX, the stretching frequency of the Li-N_2 system gives a band around 13 cm^{-1}, whereas quantum chemical calculations predict modes at higher frequencies. The transport diffusivity of oxygen is larger than the one of nitrogen. The corrected diffusivities vary with the fractional occupancy, reflecting different intermolecular forces.

References

Bär, N.K., P.L. McDaniel, C.G. Coe, G. Seiffert, and J. Kärger, *Zeolites*, **18**, 71–74 (1997).

Becke, A.D., *Phys. Rev.*, **A38**, 3098–3100 (1988).

De Luca, G., A. Arbouznikov, A. Goursot, and P. Pullumbi, *J. Phys.Chem.*, **B105**, 4663–4668 (2001).

DMol: Molecular modeling software, *Accelrys Inc.*, San Diego, USA.

Feuerstein, M. and R.F. Lobo, *Chem. Mater.*, **10**, 2197–2204 (1998).

Jale, S.R., M. Bülow, F.R. Fitch, N. Perelman, and D. Shen, *J. Phys. Chem.*, **B104**, 5272–5280 (2000).

Jobic H., J. Kärger, and M. Bée, *Phys. Rev. Lett.*, **82**, 4260–4263 (1999).

Kärger, J. and D.M. Ruthven, *Diffusion in Zeolites and Other Microporous Solids*, Wiley, New York, 1992.

Papadopoulos, G.K., H. Jobic, and D.N. Theodorou, *J. Phys. Chem.*, **B108**, 12748–12756 (2004).

Paschek, D. and R. Krishna, *Chem. Phys. Lett.*, **342**, 148–154 (2001).

Perdew, J.P., *Phys. Rev.*, **B33**, 8822–8824 (1986).

Plevert, J., F. DiRenzo, F. Fajula, and G. Chiari, *J. Phys. Chem.*, **B101**, 10340–10346 (1997).

Pullumbi, P., J. Lignieres, A. Arbouznikov, and A. Goursot, in *Metal-Ligand Interactions in Chemistry, Physics and Biology*; N. Russo (Ed.), pp. 393–451, NATO ASI Series; Plenum, New York, 1999.

Ruthven, D.M. and Z. Xu, *Chem. Eng. Sci*., **48**, 3307–3312 (1993).

Tielens, F. and P. Geerlings, *J. Mol. Catal.*, **A166**, 175–187 (2001).